Minor-Groove Recognition of Double-Stranded RNA by the Double-Stranded RNA-Binding Domain from the RNA-Activated Protein Kinase PKR†

Philip C. Bevilacqua and Thomas R. Cech*

Department of Chemistry and Biochemistry, Howard Hughes Medical Institute, University of Colorado, Boulder, Colorado 80309-0215

Received March 25, 1996; Revised Manuscript Received May 15, 1996⊗

ABSTRACT: The human double-stranded RNA- (dsRNA) activated protein kinase (PKR) has a dsRNA-binding domain (dsRBD) that contains two tandem copies of the dsRNA-binding motif (dsRBM). The minimal-length polypeptide required to bind dsRNA contains both dsRBMs, as determined by mobility-shift and filter-binding assays. Mobility-shift experiments indicate binding requires a minimum of 16 base pairs of dsRNA, while a minimal-length site for saturation of longer RNAs is 11 base pairs. Bulge defects in the helix disfavor binding, and single-stranded tails do not strongly influence the dsRNA length requirement. These polypeptides do not bind an RNA−DNA hybrid duplex or dsDNA as judged by either mobility-shift or competition experiments, suggesting 2′-OH contacts on both strands of the duplex stabilize binding. Related experiments on chimeric duplexes in which specific sets of 2′-OHs are substituted with 2′-H or 2′-OCH_3 reveal that the 2′-OHs required for binding are located along the entire 11 base-pair site. These results are supported by Fe(II) EDTA footprinting experiments that show protein-dependent protection of the minor groove of dsRNA. The dependence of dsRNA−protein binding on salt concentration suggests that only one ionic contact is made between the protein and dsRNA phosphate backbone and that at physiological salt concentrations 90% of the free energy of binding is nonelectrostatic. Thus, the specificity of PKR for dsRNA over RNA−DNA hybrids and dsDNA is largely due to molecular recognition of a network of 2′-OHs involving both strands of dsRNA and present along the entire 11 base-pair site.

Ribonucleoprotein (RNP) complexes are involved in many biological processes including transcription, posttranscriptional processing, gene regulation, translation, nucleocytoplasmic transport, and mRNA stability. In recent years, the identification of conserved sequences for RNA-binding proteins has led to the description of RNA-binding motifs (RBMs), including the double-stranded RNA- (dsRNA) binding motif (dsRBM) (Mattaj, 1993; Burd & Dreyfuss, 1994). The dsRBM was initially identified as a conserved stretch of 65−68 amino acids on the basis of sequence alignment of functionally diverse proteins from a wide range of organisms (St Johnston et al., 1992). A recent search has identified 44 dsRBM sequences from 27 proteins (Kharrat et al., 1995); these include PKR, the *Drosophila* staufen protein required for mRNA localization in the egg, the *Escherichia coli* dsRNA nuclease RNase III, and the mammalian dsRNA−adenosine deaminases (dsRADs) (Kim et al., 1994; O'Connell et al., 1995; Melcher et al., 1996).

The RNA-binding properties of polypeptides derived from the human dsRNA-dependent protein kinase PKR (also termed dsI or DAI for the dsRNA-activated inhibitor) are studied here. PKR is an interferon-induced, viral-response agent that undergoes dimerization and autophosphorylation in the presence of dsRNA, leading to dsRNA-independent phosphorylation of the eukaryotic translation initiation factor eIF-2 and inhibition of translation. More recent work indicates that PKR is involved in normal control of cell growth and differentiation and in regulation of the transcription of specific genes by dsRNA [reviewed in Clemens (1992), Hovanessian (1993), Mathews (1993), Samuel (1993), and Proud (1995)].

Like other RBMs, the dsRBM is modular and can be found in single or multiple copies in a single protein. PKR contains two tandem, N-terminal copies of the dsRBM, designated dsRBM1 and dsRBM2, and a C-terminal kinase domain (Katze et al., 1991; Feng et al., 1992; Green & Mathews, 1992; McCormack et al., 1992; Patel & Sen, 1992). dsRBM1 closely matches the dsRBM consensus sequence, while dsRBM2 matches the consensus sequence primarily in its C-terminal part (St Johnston et al., 1992). In addition, mutagenesis studies indicate that dsRBM1 is more important than dsRBM2 for dsRNA binding (Green & Mathews, 1992; McCormack et al., 1994; Green et al., 1995; Romano et al., 1995).

Structural details of protein−RNA interaction are well understood for several sequence-specific RBDs. The best characterized complex involves the RNP domain from the spliceosomal protein U1A complexed with a 21-nucleotide RNA hairpin. The crystal structure reveals the RNP making detailed sequence-specific contacts with seven nucleotides in the hairpin loop (Oubridge et al., 1994). Structures of other RNA−protein complexes also reveal sequence-specific interaction with RNA, including a bacteriophage MS2 coat protein−19-nucleotide RNA fragment complex (Valegård et al., 1994), several tRNA synthetase−tRNA complexes (Rould et al., 1989; Ruff et al., 1991), and TAR−arginine and TAR−peptide complexes (Puglisi et al., 1992, 1995; Aboul-ela et al., 1995; Ye et al., 1995). The RNAs in these

† This work is supported by a fellowship to P.C.B. from the Jane Coffin Childs Memorial Fund for Medical Research. T.R.C. is an Investigator of the Howard Hughes Medical Institute and a Professor of the American Cancer Society.

* Author to whom correspondence should be addressed.

⊗ Abstract published in *Advance ACS Abstracts,* July 15, 1996.

S0006-2960(96)00725-8 CCC: $12.00

complexes have bulges or loops that can distort the dsRNA helix, opening and widening the usually deep and narrow inaccessible major groove (Weeks & Crothers, 1993). Since the major groove contains most of the sequence-specific information, bulges render the RNA accessible to sequence-specific protein interactions (Mattaj, 1993; Steitz, 1993; McCarthy & Kollmus, 1995).

In contrast to the above examples, undistorted A-form dsRNA has its sequence-rich information buried in the major groove (Saenger, 1984; Steitz, 1993). Indeed, no sequence specificity has been observed in interactions between dsRBDs and RNA *in vitro* (Hunter et al., 1975; Manche et al., 1992; Polson & Bass, 1994; Schweisguth et al., 1994; Bycroft et al., 1995a). Furthermore, PKR does not make important contacts to bases when it binds adenovirus inhibitory RNA (VA RNA_I) (Clarke & Mathews, 1995). Recognition of dsRNA is thus likely to be novel and to involve a network of sequence-independent interactions. In this paper, we examine the roles of non-sequence-specific dsRNA functional groups, including 2′-OHs and phosphates, in binding to polypeptides and present a model to account for this binding.

MATERIALS AND METHODS

Expression and Purification of PKR Protein Constructs. C-Terminal deletion protein constructs were prepared without a $(His)_6$ tag, with an N-terminal $(His)_6$ tag, or with a C-terminal $(His)_6$ tag. Protein constructs without a $(His)_6$ tag were a gift (P. DuCharme and S. C. Schultz, personal communication). The cDNA for PKR was obtained from plasmid pB1 Nde P1 KIN (Thomis et al., 1992). Protein constructs with a C-terminal $(His)_6$ tag were prepared as follows. PCR was used to (1) introduce a recognition site for *Eco*RI 5′ to PKR coding sequences and (2) add six histidine codons, alternating between CAC and CAT codons; the stop codon, TAA; and a *Bam*HI site 3′ to PKR coding sequences. Since the coding sequences contain an internal *Eco*RI site, a complete digestion with *Bam*HI was followed by a limited digestion with *Eco*RI to allow for approximately 40% digestion. The PCR fragments were cloned into the T7 expression plasmid PKT7(-H) (S. C. Schultz and T. A. Steitz, personal communication) that had been digested with *Eco*RI and *Bam*HI.

Protein constructs with an N-terminal $(His)_6$ tag were prepared as follows. PCR was used to (1) introduce a recognition site for *Nde*I 5′ to PKR coding sequences and (2) add the stop codon, TAA, and a *Bam*HI site 3′ to PKR coding sequences. The PCR fragment was digested to completion first by *Nde*I and second by *Bam*HI. The fragment was cloned into the T7 expression plasmid pET-14b (Novagen) that contains sequences required for T7 RNA polymerase-driven overexpression, an N-terminal $(His)_6$ tag, and a thrombin restriction site for removal of the $(His)_6$ tag. Most experiments were performed with the N-terminal $(His)_6$ protein constructs. pET-14b offers the advantage that the cloning sites, *Bam*HI and *Nde*I, do not occur in the PKR coding region, allowing for rapid cloning. Sequences were confirmed by dideoxy sequencing.

Optimal expression of C-terminal deletion protein constructs was in *E. coli* strain BL21(DE3). Cells were grown at 37 °C for 12 h in LB media supplemented with 20 mM potassium phosphate (pH 7.8), 5 mM glucose, and 200 μg/mL ampicillin. Cells (5 mL) were centrifuged at 6000 rpm for 10 min, resuspended in 5 mL of LB, and diluted into 750 mL of the above media without glucose. Growth was continued at 37 °C with vigorous shaking in 2-L baffle flasks until $OD_{600} = 0.3$. The flasks were then shaken at 22 °C until $OD_{600} = 0.6-0.8$. Expression was induced by the addition of IPTG to 0.4 mM, and growth continued an additional 8 h at 22 °C. Cells were pelleted by centrifugation (10 min at 4000 rpm in a Beckman JA-10 rotor at 4 °C) and stored overnight at −20 °C. All subsequent purification steps were performed at 4 °C.

Protein was soluble and purified by native methods. Cells were resuspended in 20 mL of ice-cold sonication buffer [SB: 50 mM Hepes (pH 7.0), 700 mM NaCl, 10% glycerol, 5 mM 2-mercaptoethanol, 0.1 mM PMSF, and 0.05 mM benzamidine]. Lysozyme was added to 5 mg/mL, and the cells were incubated for 30 min with rotation, followed by sonication. The lysate was cleared by addition of one-tenth volume of 5% polyethyleneimine (pH 9.0; 25 000−50 000 average MW, Aldrich), inverted, incubated on ice for 15 min, and centrifuged (15 min at 10 000 rpm in a Beckman JA-20 rotor) (Schmedt et al., 1995). The supernatant was centrifuged (30 min at 38 000 rpm in a Beckman 70Ti rotor), collected, and subsequently rotated for 30 min with 4 mL of a 50% slurry of Ni^{2+}−nitrilotriacetic acid−agarose resin (Qiagen) previously equilibrated in SB. Imidazole (pH 7.0) was added to 1 mM, and the slurry was incubated another 30 min with rotating. The resin was then pelleted by centrifugation in a table-top swinging bucket rotor for 5 min, and the supernatant was removed. The resin was washed three times by resuspending in 40 mL of ice-cold SB plus 1 mM imidazole, rotating for 15 min, and pelleting. Washing was done an additional four times with wash buffer [WB: 50 mM Hepes (pH 7.0), 700 mM NaCl, 10% glycerol, 5 mM 2-mercaptoethanol, and 30 mM imidazole (pH 7.0)]. Protein was eluted by resuspending the resin in 3 mL of elution buffer [EB: 50 mM Hepes (pH 7.0), 700 mM NaCl, 10% glycerol, 5 mM 2-mercaptoethanol, and 300 mM imidazole (pH 7.0)], rotating for 15 min, pelleting, and combining the supernatants a total of four times. The supernatant was concentrated to 2 mL by ultrafiltration in a Centriprep-10 (10 kDa cutoff) (Amicon) and exchanged three times in storage buffer [StB: 25 mM Hepes (pH 7.0), 50 mM NaCl, 5% glycerol, 2.0 mM DTT, and 0.25 mM EDTA] by resuspending in 15 mL of StB and concentrating to 2 mL each time. Protein was stored at 4 °C. Glycerol was removed prior to Fe(II) EDTA mapping experiments by exchanging the buffer into StB minus glycerol.

The purity of recombinant C-terminal truncated PKR was estimated to be >90% from overloaded Coomasie blue stained protein gels. The concentration of protein was generally determined by the relative Coomasie blue staining on protein gels with lysozyme standards, while the concentration of p24, used to obtain the data in Table 1 and in Figure 1, was determined spectrophotometrically (Gill & von Hippel, 1989). In control experiments, the N-terminal $(His)_6$ tag in 184 and 220 amino acid proteins was removed by a thrombin digest as per manufacturer's instructions (Novagen).

Preparation of RNAs, DNAs, and Chimeras. TAR and dsTAR were prepared by T7 transcription reactions (5 mL) containing 40 mM Tris (pH 7.6), 15 mM $MgCl_2$, 10 mM DTT, 2 mM spermidine, 1 mM each nucleoside triphosphate, 0.75 μM annealed promoter-template, and 5000 units/mL phage T7 RNA polymerase (Milligan & Uhlenbeck, 1989) and incubated at 37 °C for 2 h. The promoter sequence was

the 23mer: 5′GAAATTAATACGACTCACTATAG3′. Samples were purified in 6% acrylamide gels/8 M urea, visualized by UV shadowing, excised from the gel, and eluted by crushing the gel slice and soaking overnight at 4 °C in TEN_{250} [TEN_{250}: 10 mM Tris (pH 7.5), 1 mM EDTA, and 250 mM NaCl]. RNA was concentrated by ethanol precipitation, washed with 70% ethanol, and quantitated spectrophotometrically.

All other RNA, DNA, and chimeric oligomers were prepared by solid-phase synthesis and deblocked as previously reported (Zaug et al., 1994). Oligomer sequences are found in the appropriate figure or figure caption. Positions of 2′-deoxy- or 2′-methoxy-substituted sugars were confirmed by a limited hydrolysis of the 5′-^{32}P-labeled chimera, followed by running a sequencing gel.

5′-^{32}P-labeled RNAs were generated by treatment with calf intestinal phosphatase (for T7 transcripts only), reacted with polynucleotide kinase and [γ-^{32}P]ATP, repurified by gel electrophoresis, excised from the gel, eluted overnight in TEN_{250} at 4 °C, ethanol precipitated, and resuspended in TE [10 mM Tris (pH 7.5) and 0.1 mM EDTA]. Labeled duplexes were prepared by annealing the 10 nM 5′-^{32}P-labeled strand with a 20-fold excess of complementary strand in TEN_{100} [TEN_{100}: 10 mM Tris (pH 7.5), 1 mM EDTA, and 100 mM NaCl] at 95 °C for 3 min and cooling on the bench for 10 min. Annealed duplexes were stored at −20 °C and used immediately after thawing at 22 °C. Control experiments showed no binding of protein to ssRNA.

Binding Assays. Dissociation constants were determined by either native-gel mobility-shift assays or by filter binding. Duplex RNA was 5′-^{32}P-labeled and present in limiting concentration relative to protein concentrations. Samples were prepared in standard binding buffer [BB: 25 mM Hepes (pH 7.5), 10 mM NaCl, 5% glycerol, 5 mM DTT, 0.1 mM EDTA, and 0.1 mg/mL herring sperm DNA (Sigma)]. Herring sperm DNA was fragmented by sonication to an average length of 3−4 kb, boiled for 10 min, and placed immediately on ice. Herring sperm DNA, or tRNA, as appropriate, was used in each mobility-shift assay to prevent sticking of the complex in the wells of the gel. The two binding methods gave similar results; however, the mobility-shift assay offered the advantage that multiple-protein−RNA complexes, important to the interpretation of the data presented here, could be directly visualized. In addition, filter binding experiments with short substrates suffered from poor retention efficiency, especially at high salt concentrations.

For the mobility shift assay, binding reactions were loaded onto a running 10% (79:1 acrylamide/bis) native gel. The gel and the running buffer contained 0.5× TBE [50 mM Tris base, 41.5 mM boric acid, and 1 mM EDTA, (final pH 8.3)]. Electrophoresis was performed for 1.5 h at 19 V/cm, at 22 °C.

Filter binding experiments were performed in a 96-well dot blot apparatus essentially as described (Wong & Lohman, 1993; Weeks & Cech, 1995) with the following differences. Nitrocellulose (Schleicher & Schuell) and Hybond N+ membranes were equilibrated in BB for 30 min at 22 °C. Wells were washed with 100 μL of BB, after which four reactions (10 μL each) were filtered. Wells were immediately washed with 100 μL of ice-cold BB.

Dissociation constants for chimera and salt dependence experiments were determined by quantifying the fraction (θ) of RNA bound with a PhosphorImager (Molecular Dynamics) and fitting by nonlinear least squares as a function of total PKR concentration (eq 1), where ϵ is the observed

$$\theta = \epsilon \frac{[\mathrm{PKR}]}{[\mathrm{PKR}] + K_\mathrm{d}} \quad (1)$$

maximum fraction bound (typically ≈0.8) and K_d is the dissociation constant. Control experiments were performed with 5 and 30 min of incubation of the binding reaction prior to loading the gel and gave similar results with the optimal fraction bound occurring at 5 min. All mobility-shift assays were thus performed with 5 min of incubation prior to loading the gel. For unsubstituted and MID-substituted chimeric duplexes which gave two band shifts, K_ds were calculated by treating bound RNA as a single species equal to the sum of both bands.

Dissociation constants for binding to TAR and dsTAR were determined by using a two-site binding model, quantifying the fraction of RNA bound in complex 1 (θ_1) and complex 2 (θ_2) with a PhosphorImager, and simultaneously fitting (θ_1) and (θ_2) to eqs 2 and 3, The interaction free energy between the two sites, a measure of cooperativity, was determined by eq 4, where the last term arises from statistical features due to a reduced number of sites for binding of the second protein (Cantor & Schimmel, 1980).

$$\theta_1 = \frac{[\mathrm{PKR}]K_{d2}}{[\mathrm{PKR}]^2 + [\mathrm{PKR}]K_{d2} + K_{d1}K_{d2}} \quad (2)$$

$$\theta_2 = \frac{[\mathrm{PKR}]^2}{[\mathrm{PKR}]^2 + [\mathrm{PKR}]K_{d2} + K_{d1}K_{d2}} \quad (3)$$

$$\Delta G_\mathrm{I} = +RT \ln \frac{K_{d2}}{K_{d1}} - RT \ln 4 \quad (4)$$

Fe(II) EDTA Mapping. Labeled chimeric duplexes were prepared by annealing a 5′-^{32}P-labeled strand with excess complementary strand, as described above. The top strand has a single-stranded tail 5′ to a 22 base-pair core, with the tail serving as an internal control. Oligomer sequences are found in the caption to Figure 6. Mapping conditions were adapted from published methods (Tullius & Dombroski, 1986). Protein without any glycerol was added and incubated for 5 min at 22 °C and 5 min on ice. $(NH_4)_2$-$Fe^{II}(SO_4)_2 \cdot 6H_2O$−$Na_2EDTA$, sodium ascorbate, and H_2O_2 were freshly prepared and added sequentially (1 μL each; 10 μL total volume) at final concentrations of 2 mM/4 mM, 10 mM, and 0.1%, respectively, and incubated on ice for 1 min. [In the absence of protein, similar amounts of RNA cleavage (≈20%) occurred at 1, 2, 10, and 30 min at 22 °C, suggesting 1 min is sufficient to obtain maximal cleavage.] Thiourea (10 mM) was added to quench the reaction. Five microliters of a formamide/0.1% SDS loading buffer was added that included 4 μM labeled strand, now unlabeled. Unlabeled strand was added to dissociate the 5′-^{32}P-labeled strand from the duplex since the duplex is of sufficient stability to remain partially formed on the denaturing gel. The mixture was heated to 65 °C for 3 min and put on ice. A 3 μL portion of the quenched reaction was loaded on a 25% (20:1 acrylamide/bis) gel/6 M urea/1× TBE that had been preelectrophoresed for a minimum of 2 h at 75 W.

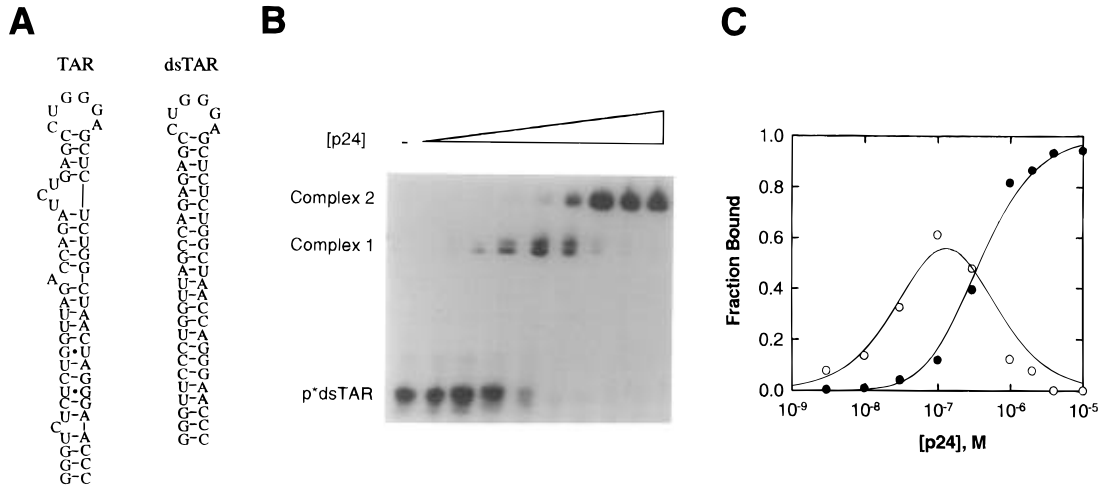

FIGURE 1: Native gel mobility shift for p24 binding to dsTAR. (A) Secondary structures for TAR and dsTAR (Celander & Cech, 1990). (B) Native-gel mobility-shift experiment for p24 binding to trace amounts of 5′-^{32}P-labeled dsTAR RNA. Experiments were in the presence of 0.1 mg/mL ssDNA. Concentrations of p24 used were 0, 0.003, 0.01, 0.03, 0.1, 0.3, 1, 2, and 4 μM. Protein binding to dsTAR resulted in two complexes. Conditions were as described in the text except that samples were loaded after 1 h of preincubation at room temperature onto a 5% (79:1 acrylamide/bis) native gel. (C) Plot of fraction of RNA bound in complex 1 (○) and complex 2 (●) for p24 binding to dsTAR. Fits are to eqs 2−4 and give values of $K_{d1} = 0.05$ μM, $K_{d2} = 0.3$ μM, and $\Delta G^{o}_{I} = +0.3$ kcal/mol (Table 1).

Marker lanes were run in Fe(II) EDTA mapping experiments. G sequencing lanes were prepared by limited hydrolysis with RNase T_1 (and without RNase T_1 as a control), and all-nucleotide sequencing lanes were prepared by treatment with alkali (Donis-Keller et al., 1977).

Computer-Generated Models. A-form RNA coordinates were generated using Insight II molecular modeling software (Biosym Technologies).

RESULTS

Effect of the $(His)_6$ Fusion Tag on Binding. To determine whether use of the $(His)_6$ tag affected the outcome of these experiments, the tag was removed by a thrombin digest. $(His)_6$-free proteins showed identical K_ds, RNA length requirement, and RNA−DNA hybrid band shifts as N-terminal $(His)_6$ tag proteins. The $(His)_6$ tag was not removed for most experiments presented.

A Model System To Study RNA−dsRBD Interactions: Minimum-Length Polypeptides and a Binding Assay. RNA substrates with and without bulges were prepared. dsTAR is a double-stranded version of TAR with a 24 base-pair stem in which the three bulges are deleted and G·U wobble pairs converted to G·C base pairs (Figure 1A). We chose TAR and dsTAR as model RNAs since TAR has been reported to both activate and inactivate PKR depending on TAR concentration, suggesting TAR can bind to PKR (Gunnery et al., 1990, 1992; Roy et al., 1991; Maitra et al., 1994). Also, the TAR RNA-binding protein (TRBP), which has three dsRBMs (Kharrat et al., 1995), binds tightly to TAR RNA and dsRNAs (Gatignol et al., 1991, 1993; Park et al., 1994). These RNAs are able to support dsRNA-specific binding (Figure 1B,C; Table 1).

In order to find a minimal-length polypeptide to study, a number of C-terminal truncated constructs were examined for binding (Figure 2). Constructs that were truncated at or before residue 100 did not give binding that was specific to dsTAR over all-DNA versions of TAR (dTAR). The minimal polypeptide examined that gave RNA-specific binding was 110 amino acids in length; its binding to dsTAR, however, was very weak (Figure 2). The minimal polypeptide that gave strong RNA-specific binding as assayed by either native-gel or filter-binding experiments was 184 residues in length and contained both dsRBM1 and dsRBM2 (Figure 2). These observations are consistent with a report that a construct with residues 1−129 gave no detectable dsRNA binding but a construct with residues 1−170 bound dsRNA (Patel & Sen, 1992). The polypeptides discussed in the remainder of this paper, p20 and p24 as well as their $(His)_6$-tagged analogs, are 184 and 220 residues in length. These polypeptides contain the same PKR amino acids as previously reported constructs (Green & Mathews, 1992; Manche et al., 1992). A 1−243 truncated construct bound RNA with similar affinity as full-length PKR with a catalytic point mutation (McCormack & Samuel, 1995), suggesting C-terminal truncated constructs retain wild-type RNA-binding activity. A longer polypeptide of 280 residues, extending to the kinase domain, bound 22-base pair dsRNA but gave complex mobility shifts with multiplets of four or more bands and was not further investigated (Figure 2). Stable RNA binding by the dsRBD from PKR requires both dsRBM1 and dsRBM2.

Table 1: Effects of Bulges and Competitor on RNA Binding to p24*a*

RNA	competitor (0.1 mg/mL)	K_{d1} (μM)	K_{d2} (μM)	ΔG^{o}_{I} (kcal/mol)
dsTAR	ssDNA	0.05	0.3	+0.3
dsTAR	$tRNA^{Phe}$	0.4	0.3	−1
TAR	ssDNA	3	0.07	−3.1
TAR	$tRNA^{Phe}$	6	1	−1.7

[a] Data are fit to a two-step random-order binding mechanism (see Materials and Methods). According to this model, K_{d1} reflects binding of one protein to RNA and K_{d2} reflects binding of a second protein to RNA. ΔG^{o}_{I} is an interaction free energy and estimates the cooperativity of protein binding to RNA, where negative values indicate positive cooperativity. Uncertainties are estimated at 30% in K_ds and 5% in ΔG^{o}_{I}s. There was no detectable binding to an all-deoxy version of TAR, dTAR, under identical conditions.

Effects of RNA Structure and Length on dsRBD Binding. Initial experiments compared binding of p24 to limiting amounts of 5′-^{32}P-labeled RNA in the presence of single-stranded DNA (ssDNA) and tRNA competitors. Binding of p24 to dsTAR or TAR gave rise to two shifted bands of different mobility (e.g., Figure 1B). The fast-mobility band,

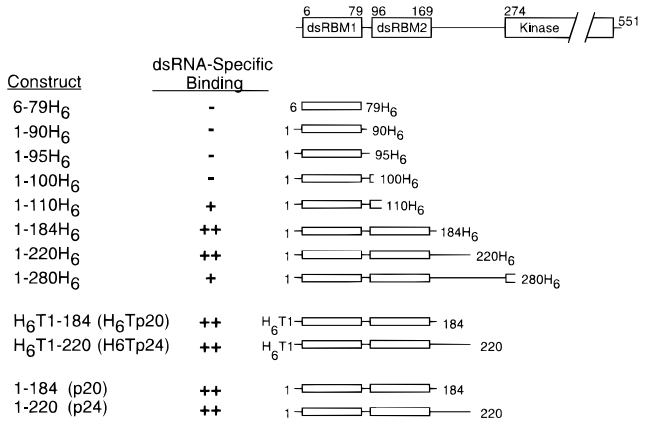

FIGURE 2: Polypeptide construct schematic. (Top) Location of dsRBM1, dsRBM2, and the kinase domain in the 551 residue PKR. dsRBM1 contains amino acids 6−79 and dsRBM2 contains amino acids 96−169 (St Johnston et al., 1992). The kinase domain resides in the C-terminal portion of PKR and contains the 11 submotifs conserved among protein kinases, with domain I starting at residue 274 (Hanks et al., 1988; McCormack et al., 1992). (Bottom) Protein constructs examined for dsRNA binding in this study. Shown are the N- and C-terminal residues of the construct, the presence of any hexahistidine tags (H_6), the presence of any thrombin cleavage sites (T), and appropriate abbreviations. dsRNA-specific binding means binding specific to TAR and dsTAR RNA over an all-DNA version of TAR (dTAR) and is indicated by (−) for no detectable specific binding and (+) for weak ($K_d \gg 1\ \mu$M) and (++) for strong ($K_d < 1\ \mu$M) binding.

complex 1, is an intermediate doublet that formed at low concentrations of p24 and was converted to the slow-migrating complex 2 at high concentration of p24. The doublet nature of complex 1 suggests a minimum of two distinct binding sites; thus a two-site random-order model was chosen to fit this data, in which one protein binds to RNA to give complex 1, followed by binding of a second protein to give complex 2 (Materials and Methods). According to this random-order binding mechanism, formation of complexes 1 and 2 is described by dissociation constants K_{d1} and K_{d2} and an interaction free energy, ΔG_I^o, that describes any cooperativity for binding of the second protein (Table 1). Complex 2 was resistant to the nonspecific protein competitor bovine serum albumin (BSA 0.5 mg/mL), suggesting complex 2 is not simply due to protein−protein aggregation (data not shown).

Table 1 summarizes the effects of adding bulges in the RNA substrate (i.e., TAR RNA) and varying the competitor. Two trends may be observed: (1) formation of complex 1 is disfavored by bulges and tRNA competitor, and (2) the interaction free energy is largest for the weakest binding combinations. The first trend is consistent with the protein−dsRNA interactions in complex 1 being weakened by bulges and subject to competition by tRNA. [In related experiments, tRNA was found to compete weakly for p20 binding to 85 base-pair dsRNA (Schmedt et al., 1995).] In addition, a stronger interaction free energy for proteins in the presence of bulges and tRNA competitor suggests that complex 2 is not as strongly affected by these factors as complex 1. The second trend is consistent with a second p24 protein binding in a cooperative fashion. This cooperativity could arise from favorable protein−protein interactions on the dsRNA, from an RNA conformational change induced by binding of the first protein, or both. One plausible RNA conformational change would involve the TAR RNA adopting a more uniform double-stranded conformation upon binding of the

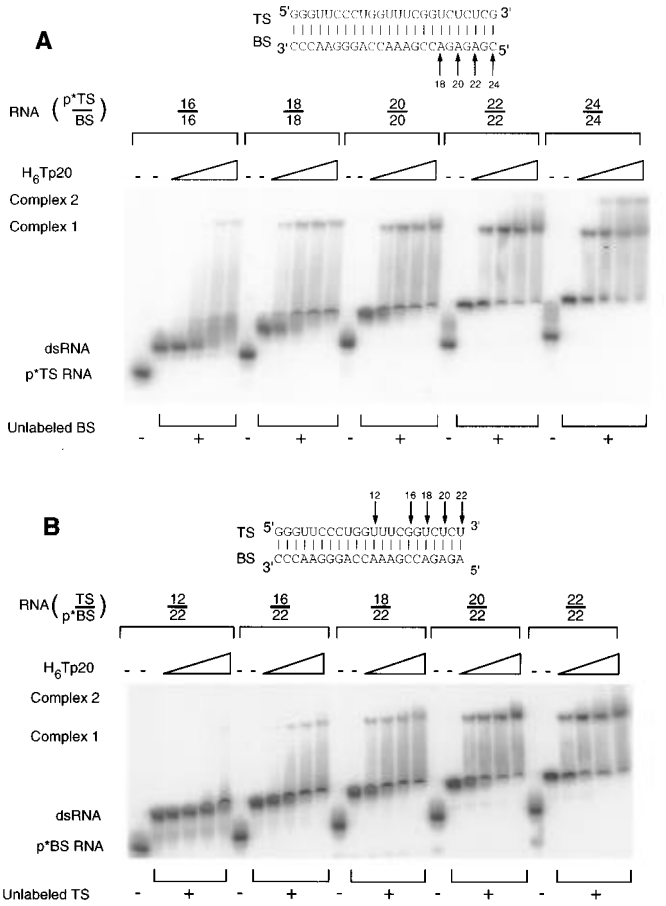

FIGURE 3: RNA length and single-stranded tail dependence. Binding of H_6Tp20 to dsRNAs of discrete length. (A) Mobility-shift experiment of H_6Tp20 binding to trace amounts of dsRNA of varying length (bp). The top-strand (TS) oligomer was 5′-^{32}P-labeled and annealed to excess amounts of unlabeled bottom-strand (BS) oligomer. Formation of dsRNA was confirmed by a microshift of p*TS upon addition of BS. [Compare (−) and (+), the first and second lanes of each RNA length set, respectively.] Sequences of TAR-derived duplexes of 18−24 base pairs are shown at the top. The sequence of 16 bp is (TS) 5′GGGUUCCCUGGUUAGC3′ and (BS) 5′GCUAACCAGGGAACCC3′. Concentrations of H_6Tp20 used were 0, 0.1, 0.3, 1, and 3 μM. Control experiments revealed no binding of 1 μM p24 to ssRNAs. (B) Mobility-shift experiments of H_6Tp20 binding to trace amounts of RNA with a double-stranded section and 5′-single-stranded tail. BS was the 22mer and was 5′-^{32}P-labeled and annealed to excess amounts of unlabeled 12-, 16-, 18-, 20-, and 22mer TS. Formation of the annealed complex was confirmed by a microshift of p*BS upon addition of TS. [Compare (−) and (+), the first and second lanes of each RNA length set, respectively.] Sequences of TAR-derived TS and BS are shown at the top. Concentrations of H_6Tp20 used were as in (A).

first molecule of p24. Subsequent experiments were performed with duplex RNA and ssDNA competitor.

Discrete-length double-stranded oligonucleotides were prepared to test directly the RNA length requirement for binding. These RNAs are derived from TAR sequences and designed to force a single base-pairing register (Figure 3A). A variety of native-gel and filter-binding conditions gave no binding of p24 to dsRNA of 6−16 base pairs, including conditions that give successful binding with longer RNAs. Moreover, binding was not observed in competition experiments in which a p*dsTAR−p24 complex was challenged with 50 μM 8 and 16 base-pair dsRNA (data not shown).

The minimal dsRNAs that bound protein were 16 base pairs for H_6Tp20 (Figure 3A) and 18 bp for p24 (data not shown). H_6Tp20 binding to 16−20 base-pair dsRNA resulted in formation of only complex 1, with complex 2

appearing for 22 and 24 base-pair dsRNA at high protein concentration. This suggests that the minimal-length site for saturation of longer RNAs is 11 base pairs (=22/2), or one turn of A-form dsRNA.

The ability of single-stranded tails to rescue binding of short double-stranded helices was also examined. As an example of the notation used, 12mer top-strand binding to the 5′-^{32}P-labeled 22mer bottom strand is called 12/22. Constructs have 5′-single-stranded overhangs. Very weak binding of H_6Tp20 to 12/22 and weak binding to 16/22 and 18/22 were observed (Figure 3B). Strong binding required 20 base pairs in 20/22. This result suggests that the dsRBD does not strongly interact with single-stranded tails, although a slight dsRNA length rescue is observed. In summary, the binding of the dsRBD from PKR requires a minimum of 16−18 base pairs of dsRNA, is not strongly rescued by single-stranded tails, and is weakened by RNAs with bulges and by tRNA competitor. In addition, the longer p24 construct shows evidence of protein−protein interaction in the presence of dsRNA.

Requirement of 2′-Hydroxyls for dsRBD Binding to dsRNA. In order to assess the role of the 2′-OH, it was first necessary to establish whether the dsRBD from PKR could bind to RNA−DNA hybrids. Mobility shifts for RNA−DNA hybrids were examined under conditions that give band shifts with an RNA−RNA duplex of identical sequence. RNA−DNA hybrids and dsDNA did not support band shifts with H_6Tp20 (Figure 4A) or p24 (data not shown), indicating that hybrids cannot bind as well as dsRNA.

It was possible, however, that hybrids could not support mobility shifts but could bind weakly to the protein. If so, hybrids should be able to compete with limiting amounts of radiolabeled dsRNA for binding to polypeptide. As shown in Figure 4B, neither dsDNA or RNA−DNA or DNA−RNA hybrids, at concentrations to 100 μM, competed effectively with trace amounts of 5′-^{32}P-labeled dsRNA for binding to H_6Tp20. Only unlabeled dsRNA itself was able to compete with release of 5′-^{32}P-labeled dsRNA. The inability of hybrids to compete was not affected by use of different buffer conditions (Figure 4B; see Discussion). The ability of the dsRBD from PKR to discriminate against RNA−DNA duplexes suggests a direct role for the 2′-OH on both strands of dsRNA in recognition of the dsRBD from PKR.

To look more closely at the 2′-OH requirement for binding, a series of chimeric duplexes was designed and their ability to bind to H_6Tp20 was tested. A 22 base-pair duplex was substituted with 2′-H or 2′-OCH_3 in 12 of 44 sugars in three different orientations: on the same face of the duplex one turn of the helix apart (SF substituted), clustered in the middle of the duplex (MID substituted), and on opposite faces of the duplex one and one-half turns apart (OF substituted) (Figure 5A). Consider first results for 2′-deoxy substitutions. Binding was strongest for the OF-substituted duplex with a K_d of 0.3 μM, compared to 0.2 μM for the unsubstituted duplex (Figure 5B). Binding to SF- and MID-substituted duplexes was somewhat weaker with K_ds of 0.6 and 2 μM, respectively. The MID-substituted duplex gave rise to two band shifts as with the unsubstituted duplex, while the SF- and OF-substituted duplexes gave primarily a single band (Figure 5B). Similar results were obtained with 2′-OCH_3-substituted chimeras (data not shown), with the OF-substituted duplex again binding tightest. Curiously, whereas MID-2′-deoxy-substituted oligomers led to two band shifts,

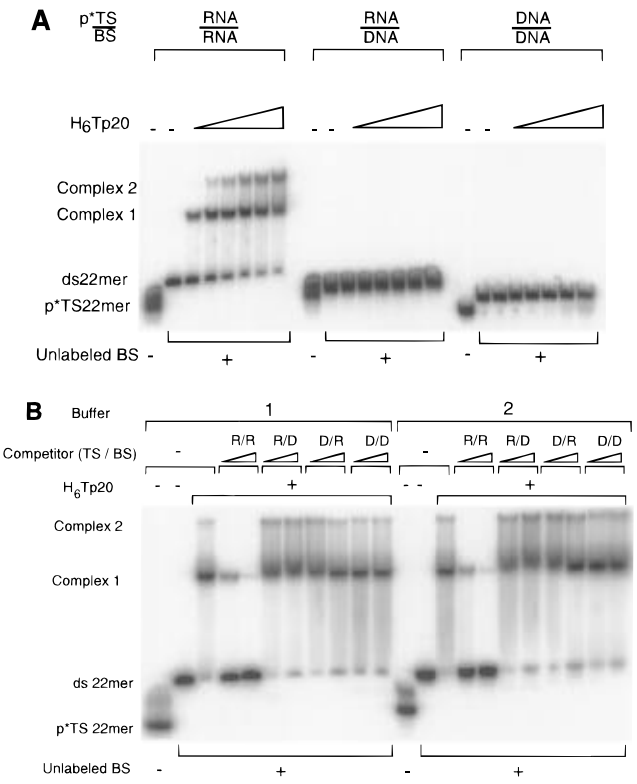

FIGURE 4: No binding of RNA−DNA hybrids or of dsDNA. (A) Mobility-shift experiment for H_6Tp20 binding to trace amounts of 22mer double-stranded nucleic acids. Top-strand (TS) oligomer was 5′-^{32}P-labeled and annealed to excess amounts of unlabeled bottom-strand (BS) oligomer. Formation of duplex was confirmed by a microshift of p*TS upon addition of BS. [Compare (−) and (+), the first and second lanes of each RNA length set, respectively.] Sequences of nucleic acids are (TS) 5′CUGGGUUCCCUGGUUUCGGUCU3′ and (BS) 5′AGACCGAAACCAGGGAACCCAG3′; rU was replaced by dU in all-deoxy strands. Concentrations of H_6Tp20 used were 0, 0.06, 0.2, 0.6, 2, 6, and 18 μM. Mobility shifts were detected only for RNA−RNA duplexes, with formation of two complexes. (B) Competition experiments for H_6Tp20 (3 μM) binding to trace amounts of 22 base-pair p*dsRNA; sequence of dsRNA as in Figure 3A. Formation of duplex was confirmed as described above. A no-competitor shift is shown in the third lane of each set. Protein was added to a mixture of trace 22 base-pair p*dsRNA and 10 or 100 μM double-stranded competitor with indicated TS/BS combinations; R = RNA and D = DNA. DNA strands are with rU replaced by dT. [Replacement of rU by rT has little effect on the activity of PKR (Baglioni et al., 1981), suggesting the difference between U and T is not significant for binding.] Buffer 1 is the 1×BB containing 25 mM Hepes (pH 7.5), 10 mM NaCl, 5% glycerol, 5 mM DTT, 0.1 mM EDTA, and 0.1 mg/mL herring sperm DNA; and buffer 2 contains 10 mM Tris (pH 8.0), 10 mM NaCl, 10% glycerol, 0.5 mM DTT, 25 mM KCl, 1 mM $MgCl_2$, 0.2 mM ATP, and 0.1 mg/mL BSA (Bass et al., 1994).

MID-2′-OCH_3-substituted oligomers led to only a single band shift.

The relative mobilities of duplexes on native gels provide information about their conformation (Bhattacharyya et al., 1990; Roberts & Crothers, 1992). Nonchimeric duplexes ran in the anticipated order dsDNA > RNA−DNA hybrid > dsRNA, and all 2′-H and 2′-OCH_3 chimeric duplexes ran similarly to each other and to dsRNA (Figure 5C). Similar mobilities of chimeric duplexes and dsRNA suggest that these duplexes have similar conformations. Thus, results with chimeric substitutions likely reflect atomic interactions and not differences in helical conformation (see Discussion).

Chemical Footprinting of the dsRBD−dsRNA Complex. To determine whether H_6Tp20 protects the minor groove of dsRNA, Fe(II) EDTA chemical footprinting experiments

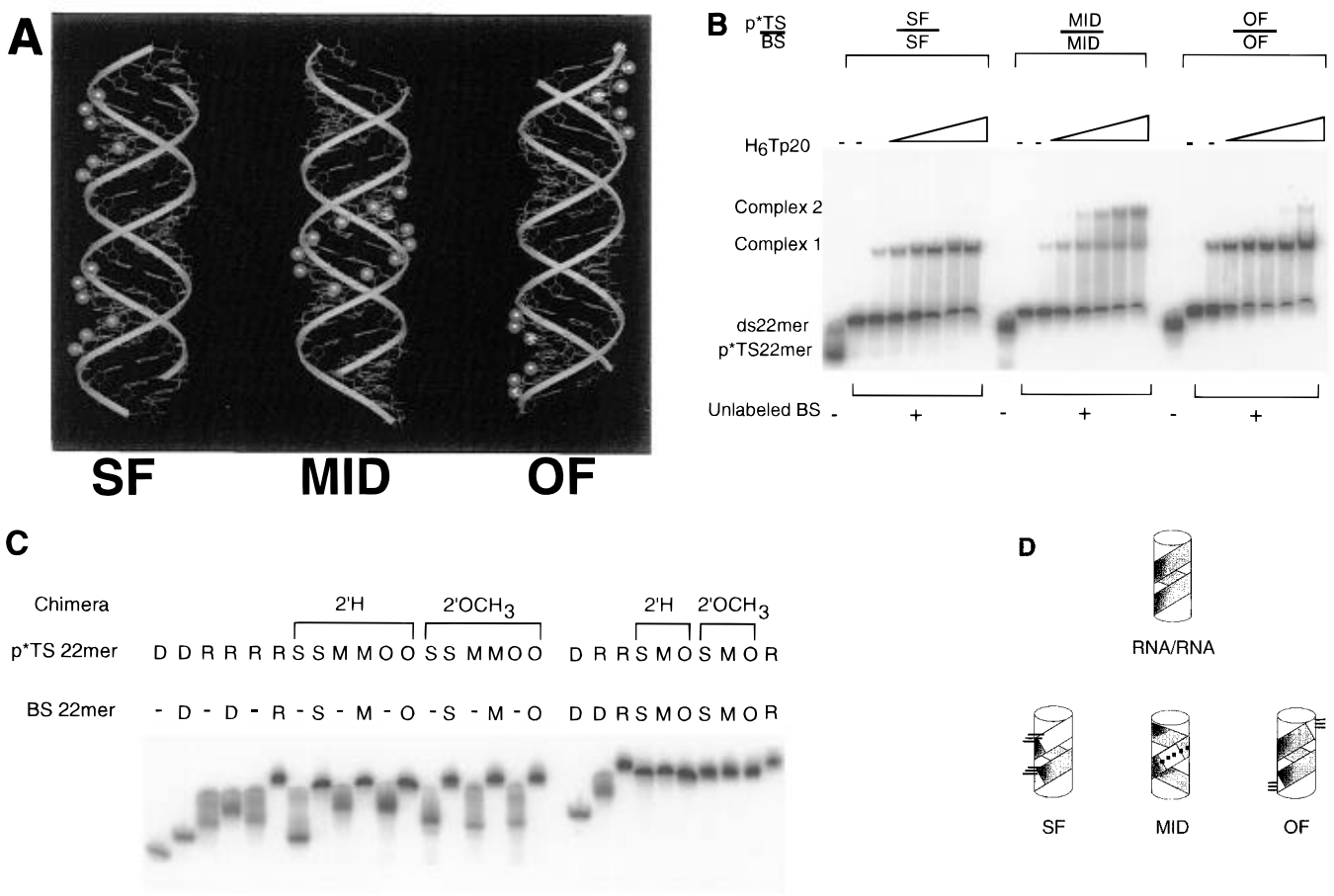

FIGURE 5: Binding of chimeras. (A) Computer-generated views of A-form 22 base-pair duplexes. Green balls show positions of 2′-deoxy substitutions. Note that the 2′-OHs are located in the wide, shallow, and accessible minor groove of A-form dsRNA. Twenty-two base pairs give two full helical turns. In each duplex, 12 of a possible 44 2′-OHs were substituted. SF = 2′-OH substitution in two sets of six on the same face (SF) of the duplex, shown on the left; MID = 2′-OH substitutions in the middle (MID) of the duplex, shown in the center; OF = 2′-OH substitutions in two sets of six on opposite faces (OF) of the duplex, shown on the right. Positions of 2′-OH substitutions for SF substitutions are in italics; MID substitutions are in lower case; and OF substitutions are underlined: top strand (TS), 5′CUGGG*UUC*-ccugguUU*CGG*UCU3′; bottom strand (BS), 5′AGAC*CGA*Aaccagg*GAAC*CCAG3′. 2′-rU is substituted with 2′-dU or 2′-OCH_3U. (B) Native-gel experiment for H_6Tp20 binding to trace amounts of duplex. Experimental conditions were the same as in Figure 4A. K_ds are 0.2 μM for RNA−RNA, 0.6 μM for SF−SF, 2 μM for MID−MID, and 0.3 μM for OF−OF. (C) Comparison of native-gel mobility of various dsRNA, 2′-H- and 2′-OCH_3-containing chimeric duplexes, and RNA−DNA hybrids. Gel conditions were the same as described in Materials and Methods for mobility-shift experiments. The left-hand portion of the gel shows confirmation of duplex formation by a microshift of p*TS upon addition of BS. (Compare the first and second lanes of each duplex set.) The right-hand portion of the gel shows relative mobility of duplexes with the RNA−RNA duplex loaded twice to provide a reference line. D = DNA, R = RNA, S = same face substituted chimeric strand, M = middle substituted chimeric strand, and O = opposite face substituted chimeric strand. (D) Model of H_6Tp20 contact on chimeric duplexes. The cylinder represents 22 bp, or two helical turns, of A-form dsRNA. The diagonal stripes represent the minor groove of the helix, the shaded stripes represent regions of contact with H_6Tp20, and each dash represents *two* deoxy sugars. The unsubstituted duplex is the minimal length of dsRNA that can accommodate two H_6Tp20s; thus its entire minor groove is shaded. The SF-substituted duplex data are consistent with the existence of one unperturbed site with 1.5 deoxy base pairs at each end. The MID-substituted duplex data are consistent with two suboptimal sites, one at each end of the duplex. The OF-substituted duplex data are consistent with six optimal sites in the center of the duplex but not with the binding of two H_6Tp20s as for the unsubstituted duplex.

were performed. Free radicals (presumably $OH^{\bullet}$) generated by solvent-based Fe(II) EDTA have been useful for probing DNA structure and RNA secondary and tertiary structure in a sequence-independent manner (Hertzberg & Dervan, 1984; Tullius & Dombroski, 1986; Latham & Cech, 1989; Celander & Cech, 1990, 1991; Murphy & Cech, 1993). In particular, the probe is thought to react with the sugar moiety of the backbone to afford strand scission (Hertzberg & Dervan, 1984; Tullius & Dombroski, 1986). Experiments on tRNA suggest the probe reports on the accessibility of the ribose 1′- and 4′-hydrogens (Latham & Cech, 1989), located in the minor groove of an A-form RNA helix. Experiments were designed with a duplex region that has chimeric OF substitutions to allow near wild-type binding and help limit the number of registers on the duplex sampled by the polypeptide. In addition, an eight-nucleotide 5′-single-stranded tail was present in some of the experiments to serve as an internal control for $OH^{\bullet}$ cleavage. Single-stranded and double-stranded regions have been shown to have similar reactivity to $OH^{\bullet}$ cleavage (Celander & Cech, 1990).

Experiments were performed with excess protein and limiting concentrations of ^{32}P-labeled duplex. Control experiments in which the RNA−protein complex was treated with cleavage reagents and then run on a native gel showed complete band shifts of nucleic acid to a single complex, identical to mobility shifts with untreated complex (data not shown). This suggests that the RNA−protein complex is stable to the cleavage conditions used.

As shown in Figure 6A, the double-stranded region was protected by H_6Tp20 from cleavage by the free-radical probe for both top- and bottom-strand 5′-^{32}P-labeled experiments. Quantitation of these experiments is shown in Figure 6B. In

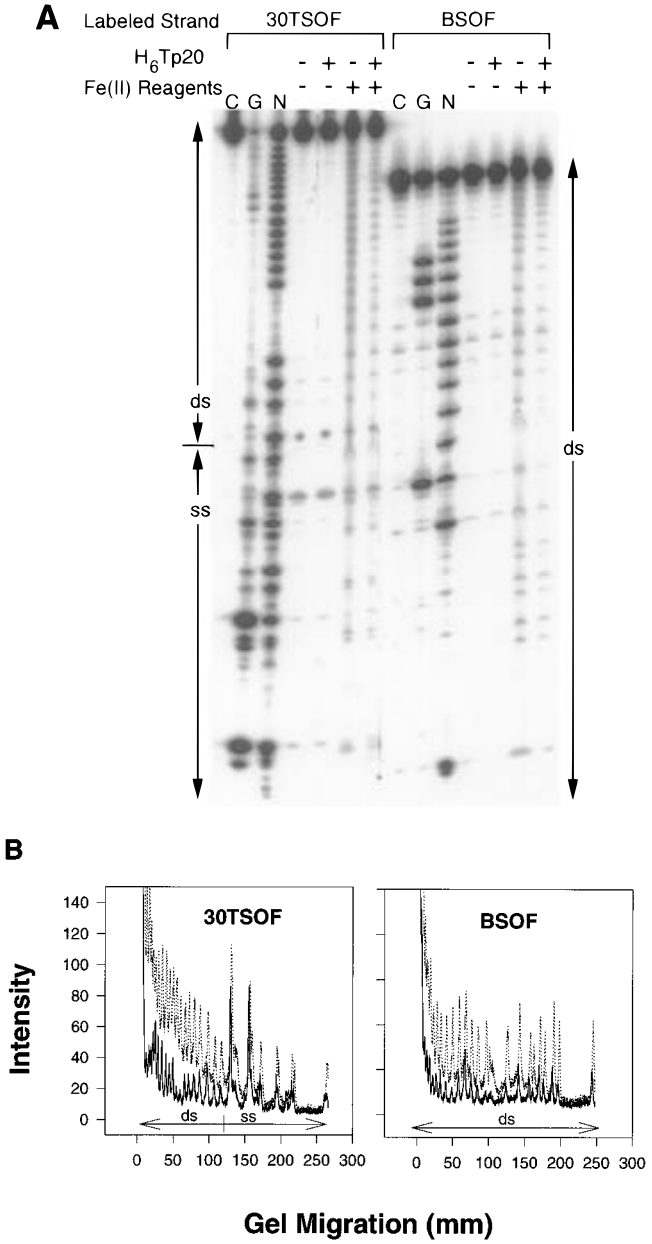

FIGURE 6: Fe(II) EDTA mapping. Fe(II) EDTA footprinting of an annealed top-strand (TS) 30mer−bottom strand (BS) 22mer complex with an eight nucleotide 5′-single-stranded end and 22 base-pair core. The core duplex is chimeric with 2′-H substitutions in the opposite face (OF) orientation. Sequences are as follows, with positions of deoxy substitution underlined: TS, 5′GGAGUGCGCUGGGUUCCCUGGUUUCGGUCU3′; BS, 5′AGACCGAAACCAGGGAACCCAG3′. (A) Denaturing 25% gel showing Fe(II) EDTA mapping. A trace amount of 5′-^{32}P-labeled 30TSOF was annealed to excess BSOF (left-hand portion of the gel), and a trace amount of 5′-^{32}P-labeled BSOF was annealed to excess 30TSOF (right-hand portion of the gel). In indicated lanes, H_6Tp20 was added at 6 μM (enough to give complete mobility shift of the complex), and in indicated lanes Fe(II) reagents were added. G, C, and N are RNase T1, control T1, and alkaline digests, respectively, of the labeled strand only. Double-stranded (ds) and single-stranded (ss) regions are marked. (B) Intensity versus gel migration for the final two Fe(II) reagent-treated lanes of each radiolabeled oligomer set in (A). Minus-protein lane is represented by a dotted line (···) and plus-protein lane by a solid line (—). An equal number of cpm of radioactivity were loaded in each lane. The loading of equal amounts of radioactivity in each lane was confirmed by integration of the PhosphorImager scans.

top-strand-radiolabeled experiments, H_6Tp20 reduced the cleavage of the double-stranded region by 60%, while cleavage of the single-stranded region was reduced by only

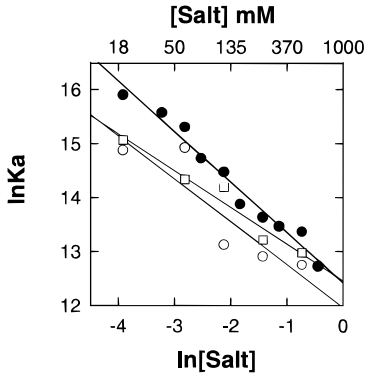

FIGURE 7: Salt dependence. Dependence of the natural logarithm of the association constant on the natural logarithm of the monovalent salt concentration for H_6Tp20 binding to 20 base-pair dsRNA; sequence as in Figure 3A. Formation of duplex was confirmed as in Figure 3, and binding to H_6Tp20 gave only a single complex. The slope gives 1.05 contacts for NaCl (●) (Record et al., 1976). Similar slopes are obtained for a NaOAc (○) and KCl (□) corresponding to 1.05 and 0.8 ion pairs, respectively.

20%. The apparent 20% protection of the single-stranded region could be due to nonspecific association of the protein with the single-stranded tail, although other effects such as quenching of free radicals by the protein could cause apparent protection. However, the 40% difference in cleavage between the double- and single-stranded regions of the RNA can be assigned to preferential protection of the double-stranded RNA by the protein. In bottom-strand-radiolabeled experiments, H_6Tp20 protected the bottom strand to a similar extent (50%). In both experiments, protection of the double-stranded region is fairly uniform, suggesting that much of the minor groove is protected by polypeptide (Figure 6B).

Determination of the Number of Ion Pairs between the dsRBD and dsRNA. Record and co-workers (1976) developed a quantitative theory that describes the number of ion pairs formed between protein and nucleic acid in terms of release of thermodynamically bound monovalent cations from the nucleic acid. A plot of ln K_a versus ln [salt] yields estimates of both the electrostatic and nonelectrostatic components of binding free energy (Record et al., 1976; Lohman et al., 1980). The slope, m, of the plot is related to the number of ion pairs, Z, between the phosphate backbone and protein by $m = -Z\Psi$, where Ψ is the fraction of counterion thermodynamically bound per phosphate. Ψ is equal to 0.89 for poly(A)·poly(U) (Record et al., 1976), and this value was used as an estimate of Ψ for the 20mer dsRNA used here.

In order to look at RNA−protein and not protein−protein interactions, binding of H_6Tp20 to 20mer dsRNA, which gives a single band shift even at high protein concentration, was studied. In addition, since divalent metal is not required for binding, it was omitted from these experiments in order to simplify the interpretation of the data. The slope for NaCl-dependence experiments is 0.94, corresponding to 1.05 (=0.94/0.89) ion pairs (Figure 7). Replacement of either the cation by K^+ or the anion by OAc^- resulted in similar dependencies (Figure 7), consistent with a general ion effect rather than an effect of specific association of either the cation or anion with the protein. Extrapolation of the fit in Figure 7 to 1 M NaCl (the y-intercept) allows calculation of the nonelectrostatic contribution to binding (Record et al., 1976; Lohman et al., 1980; Witherell & Uhlenbeck, 1989). Estimating that the ion pair destabilizes binding by 0.2 kcal/mol at 1 M NaCl (Record et al., 1976; Lohman et al., 1980),

the nonelectrostatic component of binding is −7.6 kcal/mol, accounting for approximately 90% of the total free energy of binding at physiological salt concentration.

DISCUSSION

The dsRBM is an evolutionarily conserved module which enables diverse proteins to bind dsRNA (St Johnston et al., 1992; Kharrat et al., 1995). Two recent NMR analyses of single copies of the motif revealed a structurally compact domain (Bycroft et al., 1995a; Kharrat et al., 1995). The dsRBM binds dsRNA in a sequence-independent manner (Hunter et al., 1975), suggesting that RNA recognition by the dsRBM is unique with respect to known RNP complexes. We find that the dsRBD from PKR binds dsRNA but not RNA−DNA or DNA−RNA hybrids. Our data suggest this discrimination exists because the dsRBD makes only one ion pair with the phosphate backbone, which is similar between dsRNA and hybrids, and instead largely relies on a series of nonelectrostatic 2′-OH interactions throughout the binding site involving both strands of dsRNA.

Two dsRBMs of PKR Facilitate Strong Binding of dsRNA. Native-gel and filter-binding experiments with a series of C-terminal truncated polypeptides indicate that two copies of the dsRBM from PKR are needed for strong, dsRNA-specific binding. This result contrasts with reports that polypeptides derived from PKR containing amino acids 1−91 or 1−98, having a full copy of only dsRBM1, bind to dsRNA (McCormack et al., 1992, 1994; Schmedt et al., 1995). In addition, other polypeptides containing only one copy of the dsRBM can fold into stable structures and bind dsRNA, including the third dsRBM from the *Drosophila* staufen protein, the second dsRBM from the *Xenopus* Xlrbpa protein, and the dsRBM from the *Escherichia coli* RNase III protein (St Johnston et al., 1992; Bycroft et al., 1995a,b; Kharrat et al., 1995). In the above cases, however, the polypeptide was either fused to a larger protein, complexed with an antibody, or present at high concentrations that may stabilize the protein. In addition, the dsRBM1 1−91 polypeptide binds roughly 100-fold more weakly than a polypeptide containing both dsRBMs (Schmedt et al., 1995). Requirement of tandem dsRBMs for optimal dsRNA binding has been reported previously for the *Xenopus* 4F protein (Bass et al., 1994).

dsRBD Binding Requires a Minimum of 16 Base Pairs of dsRNA. Data obtained here indicate that H_6Tp20 requires a minimum of 16 base pairs of dsRNA for strong binding to a single site on dsRNA (Figure 3A), and this requirement is not alleviated by a single-stranded tail (Figure 3B). Site-saturation experiments with H_6Tp20 indicate that two polypeptides can bind to 22 or 24 base-pair dsRNA. Ignoring looping of the RNA, overlap of protein binding sites, and dangling protein, this suggests that a single H_6-Tp20 occupies a roughly 11 base-pair site on dsRNA, equivalent to one turn of A-form dsRNA (Saenger, 1984). This observation is consistent with studies of p20 binding to a variety of longer discrete-length dsRNAs that showed that, at saturating concentrations of p20, 11 base pairs are the minimal site required for binding (Manche et al., 1992; Schmedt et al., 1995). The observation that the site size for multiple binding (11 bp) is smaller than that for single binding (16 bp) suggests that an adjacent dsRNA-bound protein can compensate for the absence of a longer dsRNA site. Initial results with a dsRBM from another protein, the third dsRBM from *Drosophila,* indicate that the minimal segment of dsRNA needed for binding is also 11 base pairs (Bycroft et al., 1995a).

Experiments with p24 binding to TAR-based oligomers indicate that bulges weaken RNA−protein interaction (Figure 2A, Table 1). Interestingly, PKR's kinase activity is not activated if an average of one mismatch is present every 8 nucleotides in RNA but can be fully activated if the mismatch occurs only once every 45 nucleotides (Minks et al., 1979). In addition, the loop and bulge of TAR are dispensable for inhibition of PKR activation (Gunnery et al., 1992), consistent with a destabilizing effect of bulges.

2′-Hydroxyls of dsRNA Are Involved in Binding. Two functional groups in dsRNA that are accessible for sequence-independent recognition by a protein are the 2′-OH and phosphate. First we will consider data on the 2′-OH. RNA−DNA hybrids, where DNA is either the top or bottom strand, and dsDNA duplexes are unable to bind to dsRBD constructs as assayed both by mobility-shift experiments and by competition experiments including 100 μM competitor duplex (Figure 4). The K_d for the all-RNA version of these hybrids binding to H_6Tp20 is 0.17 μM, and a lower limit of the K_I for the RNA−DNA hybrid is estimated at $\geq$500 μM ($=5 \times 100$ μM). These dissociation constants lead to a lower limit for the $\Delta\Delta G°$ for discrimination against RNA−DNA hybrids of $\geq$4.7 kcal/mol. Apparently, the dsRBD from PKR recognizes both strands of the dsRNA. Inability of RNA−DNA hybrids to bind to the dsRBD from PKR is consistent with the inability of such hybrids to activate PKR (Hunter et al., 1975; Sen et al., 1978).

The X*enopus* 4F protein, which contains two tandem copies of the dsRBM and a C-terminal arginine−glycine-rich block, did not support band shifts with RNA−DNA hybrids, but 100mer and 800mer hybrids were able to compete for binding at concentrations of only 50 pM (Bass et al., 1994). This competition, which is in contrast to our results with PKR, cannot be attributed to differences in solution conditions (Figure 4B); it may indicate that structural differences exist among dsRBDs as required by the specific function of the protein or that other RNA-binding motifs within a protein affect its recognition properties. The *Saccharomyces cerevisiae* RNase H protein which has two copies of the dsRBM is able to bind to hybrids; these particular motifs, however, have some variations from the conserved dsRBM (Cerritelli & Crouch, 1995).

Requirement of 2′-OHs for binding was examined further by testing a series of partially 2′-H- and 2′-OCH_3-substituted, chimeric duplexes. The unsubstituted, same-face-substituted (SF), middle-substituted (MID), and opposite-face-substituted (OF) duplexes showed only modest differences in binding (K_ds of 0.2, 0.6, 2, and 0.3 μM, respectively; Figure 5B). The more striking difference in the behavior of these duplexes is in binding stoichiometry. High H_6Tp20 concentrations led to primarily one band shift for the OF-substituted duplex, as opposed to the two band shifts observed for unsubstituted 22 base-pair dsRNA (Figures 4A and 5B). This observation suggests that H_6Tp20 binding is destabilized by deoxyriboses at the end of a binding site, contacts which would be forced on the OF-substituted duplex if it were saturated with two H_6Tp20 molecules (Figure 5D). Likewise, high H_6Tp20 concentrations led to primarily one band shift for the SF-substituted duplex (Figure 5B). This observation suggests that H_6Tp20 binding is also destabilized by deoxyriboses at the center of a binding site, interactions

which would be necessary if the SF-substituted duplex were saturated with two H_6Tp20 molecules (Figure 5D). Together, results with the OF- and SF-chimeric duplexes indicate that 2′-OHs at both the end and middle of the 11 base-pair site contribute to binding.

The destabilization of binding constants for OF- and SF-chimeric duplexes (relative to unsubstituted RNA) is only <2- and <4-fold, respectively. The small magnitude of these changes can be most readily explained by the SF-substituted duplex having one free site for H_6Tp20 binding unaffected by deoxy substitutions and the OF-substituted and unsubstituted duplexes having statistically more unsubstituted free sites. In particular, the observed K_d for binding of the first protein to a nucleic acid with multiple free sites is the K_d for binding to a single site divided by the number of free sites (McGhee & von Hippel, 1974). Observation that 16 bp is the minimal-length dsRNA for binding of a single H_6-Tp20 molecule (Figure 3A) suggests that <3 bp flanking both sides of an 11 bp ribose-containing site are needed for binding of the first protein. Given the requirement for 3 base pairs to flank each site, there are six free sites in each of the OF-substituted and unsubstituted duplexes (Figure 5D). These free sites are predicted to reduce the observed K_d for binding of the first protein to OF-substituted and unsubstituted duplexes by 6-fold relative to binding to the SF-substituted duplex, reasonably consistent with the slightly lower K_ds observed.

Binding to MID-substituted molecules led to two band shifts for the 2′-H substituted duplex and one band shift for the 2′-OCH_3-substituted duplex. The smallest contiguous dsRNA site for this molecule is 8 base pairs: there are two of these sites, one at each end of the OF-substituted duplex. Given the minimal site described for the SF-substituted duplex, the MID-substituted duplex has no free sites unaffected by deoxy substitutions with 3 flanking base pairs; there are, however, two suboptimal sites (Figure 5D). The suboptimal nature of the sites explains the 10-fold destabilization in binding. Observation of two band shifts with the 2′-deoxy-MID-substituted duplex for all but the lowest protein concentration suggests that the MID-substituted duplex achieves binding by exploiting cooperative protein−protein interactions, as observed in TAR and dsTAR experiments with the p24 construct (Table 1).

Overall, the binding constants are weaker with methoxy than with deoxy substitutions, and only a single mobility shift was observed. Weakened binding could be due to steric interference of the bulky methoxy group. Data examining PKR activation by a series of 2′-OCH_3-substituted polymeric dsRNAs (rI_n·rC_n) is consistent with these observations. Partially methylated dsRNA (<20% substituted in only one strand) fully activates PKR, while more fully methylated dsRNA (40−100% in only one strand) is unable to activate PKR (Minks et al., 1980). A single mobility shift may arise from the ability of MID 2′-OCH_3-substituted riboses to interact favorably with H_6Tp20 as hydrogen bond acceptors.

dsRNA Binding Specificity Is Not Dominated by Helix Conformation. Comparative native-gel assays report conformational differences between duplexes (Bhattacharyya et al., 1990; Roberts & Crothers, 1992). Our duplexes had relative mobilities as follows: dsDNA > RNA−DNA > 2′-OCH_3 chimeric duplexes ≈ 2′-H chimeric duplexes > RNA−RNA (Figure 5C). Relative mobilities of the non-chimeric duplexes were the same as previously reported (Bhattacharyya et al., 1990; Roberts & Crothers, 1992), indicating that this assay is able to differentiate among an A-form helix (dsRNA), a B-form helix (dsDNA), and an intermediate-form helix for the RNA−DNA hybrid (Salazar et al., 1993). Consistent with native gels reporting helix conformational information, ordering of native-gel mobility is not merely the inverse of molecular weight (i.e., dsDNA < RNA−DNA < 2′-H chimeric duplexes < dsRNA < 2′-OCH_3 chimeric duplexes). Chimeric substrates have mobilities very similar to each other and to dsRNA, suggesting an A-form-like geometry. Solution structure data on chimeric duplexes support this conclusion since the helical properties of the chimeric section of a duplex are closer to A-form than to B-form, and the RNA strand of the chimeric duplex is A-form (Zhu et al., 1995).

Since the 2′-substitutions appear to have little effect on helix geometry, it is likely that effects on binding instead reflect the disruption of atomic interactions. In addition, 10% or 20% ethanol, which can make B-form DNA and chimeric duplexes more A-form-like and rescue RNA conformationally dependent protein binding (Baidya & Uhlenbeck, 1995), had no effect on binding of dsRNA and chimeric duplexes (Bevilacqua and Cech, unpublished results), consistent with the chimera binding data reflecting true atomic interactions and not differences in helical geometry.

Minor Groove of dsRNA Is Protected by Protein. Hydroxyl-radical footprinting experiments indicate that the dsRBD protects the minor groove of dsRNA in a general manner (Figure 6), supporting direct interaction of the dsRBD with the minor groove of dsRNA. Lack of a specific H_6-Tp20 footprint, despite the presence of a chimeric background, may be due to some slippage of H_6Tp20 on the chimeric duplex due to the existence of the six overlapping binding sites (previous section). In addition, H_6Tp20 may indirectly block adjacent duplex regions from the Fe(II) EDTA probe by a steric effect. In related experiments with the adenovirus-associated VA RNA, a well-studied RNA hairpin that can inhibit PKR activation (Mathews & Shenk, 1991), three sugars in one strand of the apical stem were protected (Clarke & Mathews, 1995). Thus, in both studies recognition of dsRNA by the dsRBD appears to involve a series of minor-groove 2′-OH interactions.

Minor-groove recognition is observed in the binding of $tRNA^{Ala}$ by its aminoacyl-tRNA synthetase (Musier-Forsyth & Schimmel, 1992). Binding of RNA substrate by a group I catalytic RNA is largely sequence-independent; it involves recognition of a substrate-containing duplex by minor-groove interactions with four 2′-OHs on both strands of the duplex and the exocyclic amine of G in a terminal G·U pair [e.g., see Bevilacqua and Turner (1991), Pyle and Cech (1991), Strobel and Cech (1993, 1995)].

Small Contribution of Phosphates in dsRBD Binding to dsRNA. An experimental approach for determining the number of phosphates bound to protein by ion pairing involves a theory relating the binding constant to the ionic strength (Record et al., 1976). It has been verified experimentally for both RNA− and DNA−protein complexes. Application of this method to the R17 coat protein−RNA hairpin complex indicates 4.8 ion pairs between RNA and protein (Witherell & Uhlenbeck, 1989). The X-ray structure of a very similar RNA−protein complex shows 7 phosphates involved in 11 interactions with the protein, 5 of which involve ion pairs with the basic residues lysine and arginine and 6 of which involve polar interactions with asparagine, serine, or tyrosine, in good agreement with the solution

studies (Valegård et al., 1994) (O. C. Uhlenbeck and H. E. Johansson, personal communication). In addition, a model study involving pentalysine association with DNA indicates the theory accurately describes the number of ion pairs (Lohman et al., 1980).

Studies of specific RNA−protein complexes conclude that tat−TAR binding involves 6 ion pairs (Weeks & Crothers, 1992), R17 coat protein−RNA hairpin binding involves 4−5 ion pairs (Witherell & Uhlenbeck, 1989), U1A RBD−RNA hairpin binding involves at least 5−7 ion pairs (Hall, 1994), and S4−α mRNA binding involves at least 4 ion pairs (Deckman et al., 1987). Considering nonspecific DNA−protein complexes, gene 32 protein binds to native or ssDNA with 2 ion pairs (Jensen et al., 1976), RNase binds to denatured DNA with 7 ion pairs (Jensen & von Hippel, 1976), and *lac* repressor binds to nonspecific DNA with 12 contacts (deHaseth et al., 1977). In sharp contrast, results obtained here indicate only one ion pair in the dsRBD−dsRNA 20 base-pair complex (Figure 7). A substantial number of ionic interactions might make it difficult for a dsRNA-binding protein to discriminate against RNA−DNA hybrids and dsDNA, all of which have similar presentation of their phosphates.

Salt-dependence experiments have suggested that interaction of p20 and PKR with VA RNA involves 5 ion pairs (Clarke et al., 1994). Protection studies of p20 binding to VA RNA indicate 4 phosphates at the base of the apical stem−loop, and 3 phosphates in the complex domain are protected from iodine cleavage (Clarke & Mathews, 1995). These results contrast with observation of a single ion pair between H_6Tp20 and dsRNA observed here. There are a number of potential explanations for this difference: (1) Regions of protection from iodine cleavage may result from solvent exclusion and do not necessarily involve protein−RNA interactions (Schatz et al., 1991; Rudinger et al., 1992). (2) Some of the interactions could be nonionic, as observed in the MS2 protein−RNA complex (Valegård et al., 1994) (O. C. Uhlenbeck and H. E. Johansson, personal communication). (3) p20 may recognize VA RNA differently than dsRNA. (4) Experiments examining the salt dependence of binding to VA RNA examined only one protein concentration, so it is unclear if the data reflect equilibrium binding (Clarke et al., 1994).

Mutagenesis studies on several dsRBDs have provided results consistent with the formation of a single ion pair. Single alanine substitutions in PKR reveal only one of the conserved basic amino acids (K60) as absolutely required for binding by a solid-support poly(I)·poly(C) assay (McMillan et al., 1995), and mutagenesis studies confirm this result (Green & Mathews, 1992; Green et al., 1995). In the case of the third dsRBD from the *Drosophila* staufen protein, mutation of surface residues to alanines identifies one lysine (K50) as absolutely required for binding by a Northwestern assay (Bycroft et al., 1995a). The lysines in these two proteins occupy an equivalent position in the dsRBM-consensus sequence, situated in the loop between the third β-strand and the second α-helix in the $\alpha-\beta-\beta-\beta-\alpha$ secondary structure (Bycroft et al., 1995a), and so may have the same function in dsRNA binding. In these studies, other lysine residues were found to be important but not essential for binding, although K64 in PKR was found to be essential for dsRNA binding in other studies with a Northwestern blot analysis (McCormack et al., 1994; McCormack & Samuel, 1995).

Only dsRBM1 Appears To Contact dsRNA. K60 and K64 are conserved in both dsRBM1 and dsRBM2 (St Johnston et al., 1992); thus, if both dsRBMs were contacting the dsRNA, two ion pairs would be expected. This observation, in connection with the data of Bycroft et al. (1995a) that a single dsRBM from *Drosophila* also requires 11 base pairs of dsRNA, suggests that only one of the two dsRBMs in the dsRBD from PKR is actually contacting dsRNA. Since dsRBM1 appears to be more important than dsRBM2 for dsRNA binding (Green & Mathews, 1992; McCormack et al., 1994; Green et al., 1995; Romano et al., 1995), this suggests that only dsRBM1 directly contacts the minimal-length dsRNAs studied here. Longer dsRNAs are needed to activate full-length PKR, with 33 base pairs the minimal length and 80 base pairs the optimal length (Hunter et al., 1975; Minks et al., 1979; Manche et al., 1992). With these longer RNAs both copies of the dsRBM may contact the dsRNA leading to activation perhaps by a conformational change of the protein. The necessity of dsRBM2 for function in H_6Tp20 binding to short dsRNAs studied here may reflect protein folding requirements.

ACKNOWLEDGMENT

We thank Professor Chuck Samuel and Professor Steve Schultz for providing the plasmid DNA encoding PKR, Professor Steve Schultz and Peter DuCharme for advice on protein expression and purification and for providing purified p24, Anne Gooding and Cheryl Grosshans for oligonucleotide synthesis, Barbara Golden, Hans E. Johansson, and Joanne Bevilacqua for critically reading the manuscript, Kevin Weeks for helpful discussion, Alex Szewczak for help with computer modeling, and Professor Olke C. Uhlenbeck and Hans E. Johansson for discussion on the R17 coat protein−RNA hairpin structure.

REFERENCES

Aboul-ela, F., Karn, J., & Varani, G. (1995) *J. Mol. Biol. 253*, 313−332.
Baglioni, C., Minks, M. A., & De Clercq, E. (1981) *Nucleic Acids Res. 9*, 4939−4950.
Baidya, N., & Uhlenbeck, O. C. (1995) *Biochemistry 34*, 12363−12368.
Bass, B. L., Hurst, S. R., & Singer, J. D. (1994) *Curr. Biol. 4*, 301−314.
Bevilacqua, P. C., & Turner, D. H. (1991) *Biochemistry 30*, 10632−10640.
Bhattacharyya, A., Murchie, A. I. H., & Lilley, D. M. J. (1990) *Nature 343*, 484−487.
Burd, C. G., & Dreyfuss, G. (1994) *Science 265*, 615−621.
Bycroft, M., Grünert, S., Murzin, A. G., Proctor, M., & St Johnston, D. (1995a) *EMBO J. 14*, 3563−3571.
Bycroft, M., Proctor, M., Freund, S. M. V., & St Johnston, D. (1995b) *FEBS Lett. 362*, 333−336.
Cantor, C. R., & Schimmel, P. R. (1980) *Biophysical Chemistry*, W. H. Freeman and Co., New York.
Celander, D. W., & Cech, T. R. (1990) *Biochemistry 29*, 1355−1361.
Celander, D. W., & Cech, T. R. (1991) *Science 251*, 401−407.
Cerritelli, S. M., & Crouch, R. J. (1995) *RNA 1*, 246−259.
Clarke, P. A., & Mathews, M. B. (1995) *RNA 1*, 7−20.
Clarke, P. A., Pe'ery, T., Ma, Y., & Mathews, M. (1994) *Nucleic Acids Res. 22*, 4364−4374.
Clemens, M. (1992) *Nature 360*, 210−211.
Deckman, I. C., Draper, D. E., & Thomas, M. S. (1987) *J. Mol. Biol. 196*, 313−322.
deHaseth, P. L., Lohman, T. M., & Record, M. T., Jr. (1977) *Biochemistry 16*, 4783−4790.

Donis-Keller, H., Maxam, A. M., & Gilbert, W. (1977) *Nucleic Acids Res. 4*, 2527−2538.
Feng, G.-S., Chong, K., Kumar, A., & Williams, B. R. G. (1992) *Proc. Natl. Acad. Sci. U.S.A. 89*, 5447−5451.
Gatignol, A., Buckler-White, A., Berkhout, B., & Jeang, K.-T. (1991) *Science 251*, 1597−1600.
Gatignol, A., Buckler, C., & Jeang, K.-T. (1993) *Mol. Cell. Biol. 13*, 2193−2202.
Gill, S. C., & von Hippel (1989) *Anal. Biochem. 182*, 319−326.
Green, S. R., & Mathews, M. B. (1992) *Genes Dev. 6*, 2478−2490.
Green, S. R., Manche, L., & Mathews, M. B. (1995) *Mol. Cell. Biol. 15*, 358−364.
Gunnery, S., Rice, A. P., Robertson, H. D., & Mathews, M. B. (1990) *Proc. Natl. Acad. Sci. U.S.A. 87*, 8687−8691.
Gunnery, S., Green, S. R., & Mathews, M. B. (1992) *Proc. Natl. Acad. Sci. U.S.A. 89*, 11557−11561.
Hall, K. B. (1994) *Biochemistry 33*, 10076−10088.
Hanks, S. K., Quinn, A. M., & Hunter, T. (1988) *Science 241*, 42−52.
Hertzberg, R. P., & Dervan, P. B. (1984) *Biochemistry 23*, 3934−3945.
Hovanessian, A. G. (1993) *Semin. Virol. 4*, 237−245.
Hunter, T., Hunt, T., Jackson, R. J., & Robertson, H. D. (1975) *J. Biol. Chem. 250*, 409−417.
Jensen, D. E., & von Hippel, P. H. (1976) *J. Biol. Chem. 251*, 7198−7214.
Jensen, D. E., Kelly, R. C., & von Hippel, P. H. (1976) *J. Biol. Chem. 251*, 7215−7228.
Katze, M. G., Wambach, M., Wong, M.-L., Garfinkel, M., Meurs, E., Chong, K., Williams, B. R. G., Hovanessian, A. G., & Barber, G. N. (1991) *Mol. Cell. Biol. 11*, 5497−5505.
Kharrat, A., Macias, M. J., Gibson, T. J., Nilges, M., & Pastore, A. (1995) *EMBO J. 14*, 3572−3584.
Kim, U., Wang, Y., Sanford, T., Zeng, Y., & Nishikura, K. (1994) *Proc. Natl. Acad. Sci. U.S.A. 91*, 11457−11461.
Latham, J. A., & Cech, T. R. (1989) *Science 245*, 276−282.
Lohman, T. M., deHaseth, P. L., & Record, M. T., Jr. (1980) *Biochemistry 19*, 3522−3530.
Maitra, R. K., McMillan, N. A. J., Desai, S., McSwiggen, J., Hovanessian, A. G., Sen, G., Williams, B. R. G., & Silverman, R. H. (1994) *Virology 204*, 823−827.
Manche, L., Green, S. R., Schmedt, C., & Mathews, M. B. (1992) *Mol. Cell. Biol. 12*, 5238−5248.
Mathews, M. B. (1993) *Semin. Virol. 4*, 247−257.
Mathews, M. B., & Shenk, T. (1991) *J. Virol. 65*, 5657−5662.
Mattaj, I. W. (1993) *Cell 73*, 837−840.
McCarthy, J. E. G., & Kollmus, H. (1995) *Trends Biochem. Sci. 20*, 191−197.
McCormack, S. J., & Samuel, C. E. (1995) *Virology 206*, 511−519.
McCormack, S. J., Thomis, D. C., & Samuel, C. E. (1992) *Virology 188*, 47−56.
McCormack, S. J., Ortega, L. G., Doohan, J. P., & Samuel, C. E. (1994) *Virology 198*, 92−99.
McGhee, J. D., & von Hippel, P. H. (1974) *J. Mol. Biol. 86*, 469−489.
McMillan, N. A. J., Carpick, B. W., Hollis, B., Toone, W. M., Zamanian-Daryoush, M., & Williams, B. R. G. (1995) *J. Biol. Chem. 270*, 2601−2606.
Melcher, T., Maas, S., Herb, A., Sprengel, R., Seeburg, P. H., & Higuchi, M. (1996) *Nature 379*, 460−464.
Milligan, J. F., & Uhlenbeck, O. C. (1989) *Methods Enzymol. 180*, 51−62.
Minks, M. A., West, D. K., Benvin, S., & Baglioni, C. (1979) *J. Biol. Chem. 254*, 10180−10183.
Minks, M. A., West, D. K., Benvin, S., Greene, J. J., Ts'o, P. O. P., & Baglioni, C. (1980) *J. Biol. Chem. 255*, 6403−6407.
Murphy, F. L., & Cech, T. R. (1993) *Biochemistry 32*, 5291−5300.
Musier-Forsyth, K., & Schimmel, P. (1992) *Nature 357*, 513−515.
O'Connell, M. A., Krause, S., Higuchi, M., Hsuan, J. J., Totty, N. F. T., Jenny, A., & Keller, W. (1995) *Mol. Cell. Biol. 15*, 1389−1397.
Oubridge, C., Ito, N., Evans, P. R., Teo, C.-H., & Nagai, K. (1994) *Nature 372*, 432−438.
Park, H., Davies, M. V., Langland, J. O., Chang, H.-w., Nam, Y. S., Tartaglia, J., Paoletti, E., Jacobs, B. L., Kaufman, R. J., & Venkatesan, S. (1994) *Proc. Natl. Acad. Sci. U.S.A. 91*, 4713−4717.
Patel, R. C., & Sen, G. C. (1992) *J. Biol. Chem. 267*, 7671−7676.
Polson, A. G., & Bass, B. L. (1994) *EMBO J. 13*, 5701−5711.
Proud, C. G. (1995) *Trends Biochem. Sci. 20*, 241−246.
Puglisi, J. D., Tan, R., Calnan, B. J., Frankel, A. D., & Williamson, J. R. (1992) *Science 257*, 76−80.
Puglisi, J. D., Chen, L., Blanchard, S., & Frankel, A. D. (1995) *Science 270*, 1200−1203.
Pyle, A. M., & Cech, T. R. (1991) *Nature 350*, 628−631.
Record, M. T., Jr., Lohman, T. M., & deHaseth, P. (1976) *J. Mol. Biol. 107*, 145−158.
Roberts, R. W., & Crothers, D. M. (1992) *Science 258*, 1463−1466.
Romano, P. R., Green, S. R., Barber, G. N., Mathews, M. B., & Hinnebusch, A. G. (1995) *Mol. Cell. Biol. 15*, 365−378.
Rould, M. A., Perona, J. J., Söll, D., & Steitz, T. A. (1989) *Science 246*, 1135−1142.
Roy, S., Agy, M., Hovanessian, A. G., Sonenberg, N., & Katze, M. (1991) *J. Virol. 65*, 632−640.
Rudinger, J., Puglisi, J. D., Pütz, J., Schatz, D., Eckstein, F., Florentz, C., & Giegé, R. (1992) *Proc. Natl. Acad. Sci. U.S.A. 89*, 5882−5886.
Ruff, M., Krishnaswamy, S., Boeglin, M., Poterszman, A., Mitschler, A., Podjarny, A., Rees, B., Thierry, J. C., & Moras, D. (1991) *Science 252*, 1682−1689.
Saenger, W. (1984) *Principles of Nucleic Acid Structure*, Springer-Verlag, New York.
Salazar, M., Fedoroff, O. Y., Miller, J. M., Ribeiro, N. S., & Reid, B. R. (1993) *Biochemistry 32*, 4207−4215.
Samuel, C. E. (1993) *J. Biol. Chem. 268*, 7603−7606.
Schatz, D., Leberman, R., & Eckstein, F. (1991) *Proc. Natl. Acad. Sci. U.S.A. 88*, 6132−6136.
Schmedt, C., Green, S. R., Manche, L., Taylor, D. R., Ma, Y., & Mathews, M. B. (1995) *J. Mol. Biol. 249*, 29−44.
Schweisguth, D. C., Chelladurai, B. S., Nicholson, A. W., & Moore, P. B. (1994) *Nucleic Acids Res. 22*, 604−612.
Sen, G. C., Taira, H., & Lengyel, P. (1978) *J. Biol. Chem. 253*, 5915−5921.
Steitz, T. A. (1993) in *The RNA World* (Gesteland, R. F., & Atkins, J. F., Eds.) p 219, Cold Spring Harbor Laboratory Press, Cold Spring Harbor, NY.
St Johnston, D., Brown, N. H., Gall, J. G., & Jantsch, M. (1992) *Proc. Natl. Acad. Sci. U.S.A. 89*, 10979−10983.
Strobel, S. A., & Cech, T. R. (1993) *Biochemistry 32*, 13593−13604.
Strobel, S. A., & Cech, T. R. (1995) *Science 267*, 675−679.
Thomis, D. C., Doohan, J. P., & Samuel, C. E. (1992) *Virology 188*, 33−46.
Tullius, T. D., & Dombroski, B. A. (1986) *Proc. Natl. Acad. Sci. U.S.A. 83*, 5469−5473.
Valegård, K., Murray, J. B., Stockley, P. G., Stonehouse, N. J., & Liljas, L. (1994) *Nature 371*, 623−626.
Weeks, K. M., & Crothers, D. M. (1992) *Biochemistry 31*, 10281−10287.
Weeks, K. M., & Crothers, D. M. (1993) *Science 261*, 1574−1577.
Weeks, K. M., & Cech, T. R. (1995) *Biochemistry 34*, 7728−7738.
Witherell, G. W., & Uhlenbeck, O. C. (1989) *Biochemistry 28*, 71−76.
Wong, I., & Lohman, T. M. (1993) *Proc. Natl. Acad. Sci. U.S.A. 90*, 5428−5432.
Ye, X., Kumar, R. A., & Patel, D. J. (1995) *Chem. Biol. 2*, 827−840.
Zaug, A. J., Dávila-Aponte, J. A., & Cech, T. R. (1994) *Biochemistry 33*, 14935−14947.
Zhu, L., Salazar, M., & Reid, B. R. (1995) *Biochemistry 34*, 2372−2380.

BI9607259